
Bone Pathologic Correlation of Multimodality Imaging in Paget's Disease

Yong Whee Bahk, Young Ha Park, Soo Kyo Chung and Je Geun Chi

Departments of Radiology and Nuclear Medicine, Kangnam St. Mary's Hospital, Catholic University Medical College; and Department of Pathology, Seoul National University Hospital, Seoul, Korea

The pagetic bones in the active phase of the disease with brisk lysis and sclerosis manifest intense tracer uptake on planar bone and SPECT images. Intense tracer uptake, however, can occur also in infections, dysplasias and metastases. Pinhole bone scintigraphy has been shown to portray specific diagnostic signs in a number of skeletal diseases. In an effort to identify useful bone scan signs, we prospectively carried out ^{99m}Tc -oxidronate pinhole bone scintigraphy of the skull, vertebrae, ribs, humerus, sacrum and ilium in two patients with Paget's disease of the bone. The pinhole bone scintigraphy findings correlated with radiographic, CT and MRI findings and in the vertebra with the pathological study. Interestingly enough, pinhole bone scintigraphy revealed intense tracer uptake preferentially in the bone cortex and the rim of the affected bones. Thus, the cranial inner table, humeral cortex and vertebral endplates and rims were the seats of characteristic tracer uptake, respectively creating a scintigraphic version of the radiographic "cotton wool" sign, "casket" sign and "picture frame" sign. The pagetic lesions in the sacrum and ilium also showed intense cortical and rim uptake. Correlation of pinhole bone scintigraphy with radiography, CT and MRI indicated that such cortical or rim uptake is characteristic of Paget's disease.

Key Words: Paget's disease; osteitis deformans; pinhole bone scintigraphy

J Nucl Med 1995; 36:1421-1426

Most cases of the highly prevalent Paget's disease of the bone are polyostotic, although this disease can be monostotic in 10%–35% of patients (1). The preferred sites are the skull, spine, pelvis, humerus, femur, rib and scapula (1–3). Radiography is the primary diagnostic tool, but some of the polyostotic lesions may escape detection because whole-body radiography is not easily performed and at times is incomplete. Because of its high sensitivity, ^{99m}Tc -diphosphonate (HDP) bone scanning is widely used for screening (3–7) as well as therapeutic management of Paget's disease (3, 8, 9). The planar bone scan shows hot areas, often extreme in intensity, in the skull, axial skele-

ton and limbs (6, 10). Understandably, however, the individual hot areas seen on the planar and SPECT images lack specificity of topography and texture, which diminishes their value. The list of the radiographic differential diagnoses of sclerotic bone lesions, including Paget's disease, is redundant (11); multiple hot areas are all too common in many polyostotic diseases, such as multifocal infections, dysplasias and metastases, and a single hot area is not less common to other bone diseases. Pinhole bone scintigraphy is useful to diagnose many bone diseases because it can portray anatomic, textural and pathochemical alterations in much greater detail (12–21).

Pathologically, the pagetic bone in the active phase of the disease is characterized by brisk osteoclastic and osteoblastic activities with trabecular resorption and apposition, increased vascularity and fibrous replacement of the bone marrow (2, 7, 22). Such bone changes are known to predispose in the cortex of the axial and limb bones and the cranial tables, manifesting porous sclerosis due to woven bone formation that resembles pumice bone (2, 22). Thus, it appears to be essential from a diagnostic imaging standpoint to demonstrate typical pagetic bone change in the cortex of the preferred bone, as well as bone enlargement and marrow-space alterations (1, 24–26).

Our study was conducted to prospectively determine bone scan features that reflect the pathologic changes in Paget's disease as previously described. Pinhole bone scintigraphy was performed in the bones affected with Paget's disease, and these alterations were correlated with those from radiography, CT scan and MRI, and with pathological changes in the vertebra.

CASE REPORT

Materials

Six different bones from two patients (a 57-yr-old woman and a 67-yr-old man) with Paget's disease were investigated. The skull, right humerus and sacrum were affected in the first patient and the thoracic spine, ribs and left ilium in the second. Imaging studies included plain bone radiography and both planar and pinhole bone scintigraphy for all six sites. In addition, MRI was performed for the cranial lesion in Patient 1 and CT, MRI and biopsy of the vertebral lesion in Patient 2.

Methods

Bone scans were obtained following intravenous injection of 0.74 GBq (20 mCi) of ^{99m}Tc -HDP. The whole-body scan was

Received June 13, 1994; revision accepted Sept. 20, 1994.
For correspondence or reprints contact: Yong Whee Bahk, MD, Department of Radiology and Nuclear Medicine, Kangnam St. Mary's Hospital, Catholic University Medical College, Banpodong, Sochoku, Seoul, 137-040 Korea.

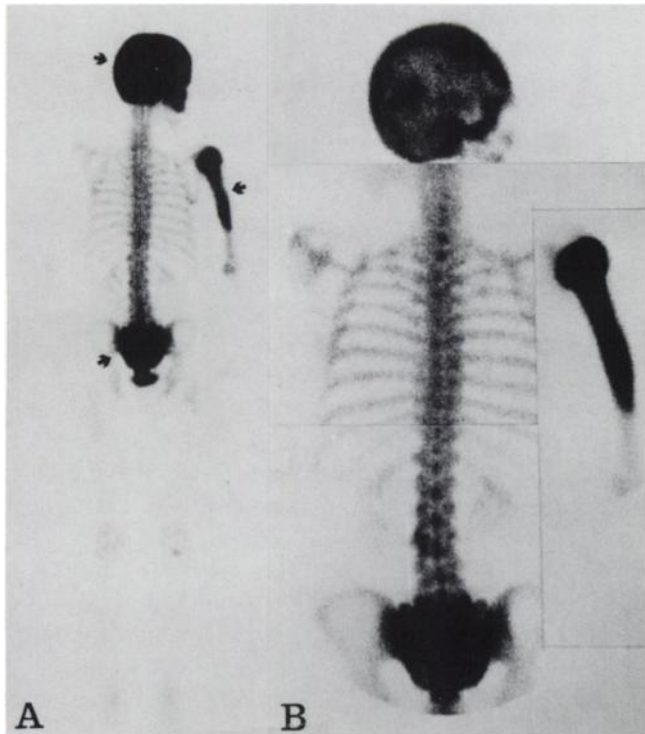


FIGURE 1. Whole body in Patient 1. (A) Posterior whole-body scan and (B) composite high-resolution spot view show intense tracer uptake in the skull, right humerus and sacrum (arrows). In general, the uptake appears simply intense and homogeneous. Despite the significantly improved resolution, the spot view fails to portray topographic detail and subtle change sufficiently to permit piecemeal analysis of pathology (Cf. Figs. 2A, 3A, and 4A).

started 2 hr postinjection. Planar spot views and pinhole bone scintigraphs were then acquired on each of the abnormal bones. A total of 450K cts were accumulated per scan. The time spent on each scan ranged from 15 to 20 min. A Siemens (Des Plaines, IL) Scintiview II or Orbiter camera was used with a 4-mm pinhole

collimator. Radiography, CT and MRI were carried out according to standard bone techniques.

Observation

The initial observation included baseline reading of the planar and pinhole bone scans and correlation of the bone scans with radiographs in all six lesion sites. We then cross-correlated the findings shown on: (a) pinhole bone scintigraphy, radiography and MRI of the skull with the classic radiographic “cotton wool” sign in Patient 1; and (b) pinhole bone scintigraphy, radiography, CT, MRI, and pathological evaluation of the vertebra in Patient 2, whose radiograph showed a typical picture frame sign.

Patient 1

In March 1993, a 57-yr-old woman was admitted for the evaluation of right humeral pain that had persisted for months. In 1987, she underwent left mastectomy for breast cancer; the bone scans obtained at that time and in the following years as a part of the cancer staging and follow-up protocol repeatedly revealed intense tracer uptake in the skull, right humerus and sacrum (Fig. 1A). Scintigraphically, the diagnosis of Paget’s disease was already suggested, but nothing had been done to obtain a more complete diagnosis. Physical examination revealed mild bony protrusion in the forehead and right upper arm. Complete blood count and urinalysis were within normal limits. Blood chemistry showed marked increase in alkaline phosphatase (2138). Acid phosphatase, calcium and phosphate were all within normal range.

A whole-body bone scan obtained at admission again revealed intense tracer uptake but without textural detail (Fig. 1A). Basically, the scan alterations had remained unchanged since the initial study. High-resolution spot views showed much improved resolution. Nevertheless, they also failed to show accurate topography and textural details sufficiently clear to permit specific diagnosis, except in the sacrum (Fig. 1B). Resolution did not improve at all in the humerus. Supplementary pinhole bone scintigraphy portrayed preferential tracer uptake characteristically in the cortex or rim in all affected bones. Thus, pinhole bone scintigraphy of the skull showed an area of more intense uptake against less intense background uptake in the inner table and

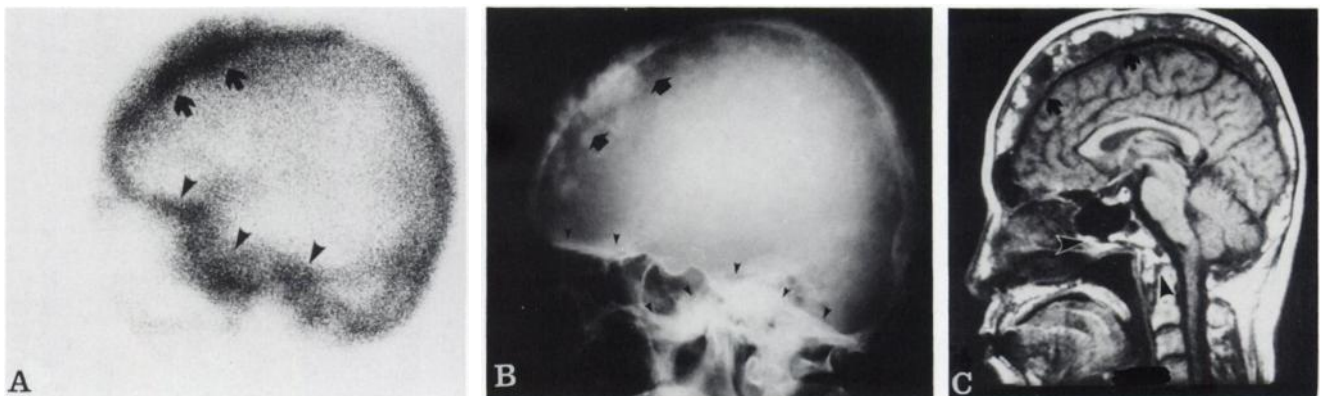


FIGURE 2. Skull in Patient 1. (A) Lateral pinhole scan portrays diffuse, intense tracer uptake in the vault and base (arrowheads) with the most pronounced uptake localized in the frontal inner table and diploe (arrows). (B) Lateral radiograph shows a classic cotton wool sign with lysis, most typically in the frontoparietal regions (arrows) and sclerosis in the base (arrowheads). The diploic space is expanded and lytic and the outer table porotic (not well reproduced due to the high-penetration technique). (C) T1-weighted midsagittal MRI demonstrates diploic widening and the deposition of abnormal tissues having intermediate and high signal intensities. Similar change can be seen in the skull base (arrowheads). The most pronounced change again occurs in the frontal region (arrows). Notice the close correlation among pinhole bone scintigraphy change, radiographic cotton wool sign and MRI alterations, all denoting brisk lysis and new bone formation in Paget’s disease.

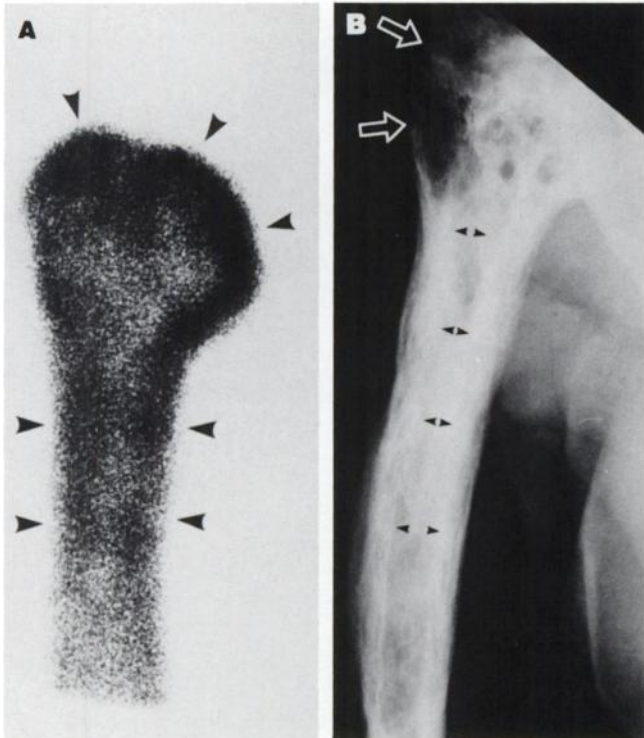


FIGURE 3. Right humerus in Patient 1. (A) Anterior pinhole bone scan portrays intense tracer uptake preferentially in the cortices of the head, neck, and shaft (arrowheads) with the most pronounced change occurring in the humeral head. The marrow space is encroached upon and relatively photopenic. (B) Anteroposterior radiograph shows cortical thickening with pumice-bone change in the head and neck (open arrows) and shaft (arrow). The affected bone is enlarged and marrow space encroached upon (paired arrowheads).

diploe of the frontal bone (Fig. 2A). The comparison with the skull radiograph revealed that the more intense, patchy uptake corresponds to the most pronounced cotton wool change (Fig. 2B). The diploic space was expanded and the outer table was porotic, lytic and irregularly thickened; the skull base was also diffusely thickened. Midsagittal T1-weighted skull MRI revealed intermediate signal intensities irregularly intermingled with high signal intensities in the frontal diploe that was expanded, denoting the deposition of the pagetic tissue and fat (Fig. 2C). The inner table was thickened. Such MRI alterations closely correlated with the cotton wool sign seen on pinhole bone scintigraphy (Fig. 2A) and radiography (Fig. 2B). In the right humerus, the tracer uptake was intense and preferential in the cortices of the head, neck, and shaft with the most pronounced change occurring in the head (Fig. 3A). Radiographically, the humeral head, neck and shaft showed diffuse cortical thickening with classic pumice-bone change (Fig. 3B). The affected bone was enlarged and the marrow space encroached upon, creating a classic casket sign. Posterior pinhole bone scintigraphy of the sacrum portrayed similar, preferential uptake in the cortices of the crests, spines, edges and intervertebral foramina, which were enlarged (Fig. 4A). Anteroposterior radiographic view of the sacrum showed comparable sclerosis in the cortices of the anatomical parts mentioned above, including enlarged foramina (Fig. 4B). Based on all these imaging studies and blood chemistry, a diagnosis of Paget's disease was made.

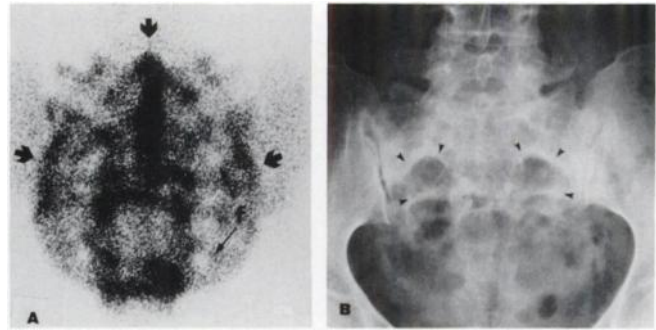


FIGURE 4. Sacrum in Patient 1. (A) Posterior pinhole bone scan portrays intense tracer uptake preferentially in the lateral edges, crests, spinous tubercles (arrows), and dilated intervertebral foramina (f). (B) Anteroposterior radiograph shows irregularly thickened cortices and disorganized trabeculae with increased bone size. The alterations are more pronounced in the lateral edges, crests, spinous tubercles, and intervertebral foramina (arrowheads). Notice the close correlation between the scintigraphic and radiographic alterations.

Patient 2

In March 1993, a 67-yr-old man was admitted to evaluate dorsal pain of many years duration and a radiating pain in the left anterior chest which had persisted irregularly for a year. Four years earlier, in another hospital, he underwent laminectomies of T4–T7 to relieve stenosis caused by thickened vertebrae, but no pathological study was done at that time. Clinical inspection confirmed an incision scar over the midthoracic spine and the thoracolumbar junction was tender. Complete blood count and urinalysis were within normal limits. Blood chemistry showed markedly increased serum alkaline phosphatase (4290) and 24-hr urine showed markedly elevated hydroxyproline level (free = 18.00 μ mole/day; total = 1335 μ mole/day). Serum acid phosphatase, calcium, and phosphate were within normal range.

Admission radiographs of the thoracic spine showed diffuse, irregular, vertebral sclerosis with a midline laminectomy defect in T4–T7, the classic picture frame sign in T10 and T11 and a compression fracture of T9 (Fig. 5A). Some of the midthoracic ribs showed irregular, trabecular thickening. Radiography strongly suggested Paget's disease, and further imaging tests, including bone scanning, were performed. A high-resolution planar bone scan showed intense tracer uptake in the thoracic spine and ribs as well as in the left sacroiliac joint region. The uptake was intense and diffuse with no textural details (Fig. 5B). A small, photopenic defect was seen in the midthoracic spine, denoting previous laminectomy. Pinhole bone scintigraphy was performed to obtain more detailed observation and portrayed individual vertebrae rather distinctly (Fig. 5C). Typically, T10 and T11 vertebrae showed intense uptake in the endplates and lateral rims, giving rise to a rimmed appearance, a scintigraphic version of the radiographic picture frame sign (Fig. 5A). The vertebrae were enlarged and spinal foramina stenotic. Vertebra T9 was reduced in height, reflecting fracture. Affected ribs showed diffuse and segmental uptake, which were not localized. Transaxial CT of vertebra T10 demonstrated bizarre trabecular thickening with the most prominent change occurring in the cortex, which are typical of Paget's disease (Fig. 5D). Midsagittal T1-weighted MRI showed irregular replacement of marrow with intermediate and high signal intensities, denoting Paget's disease (Fig. 5E). Because of the incidental finding of intense tracer uptake in the left ilium on planar bone

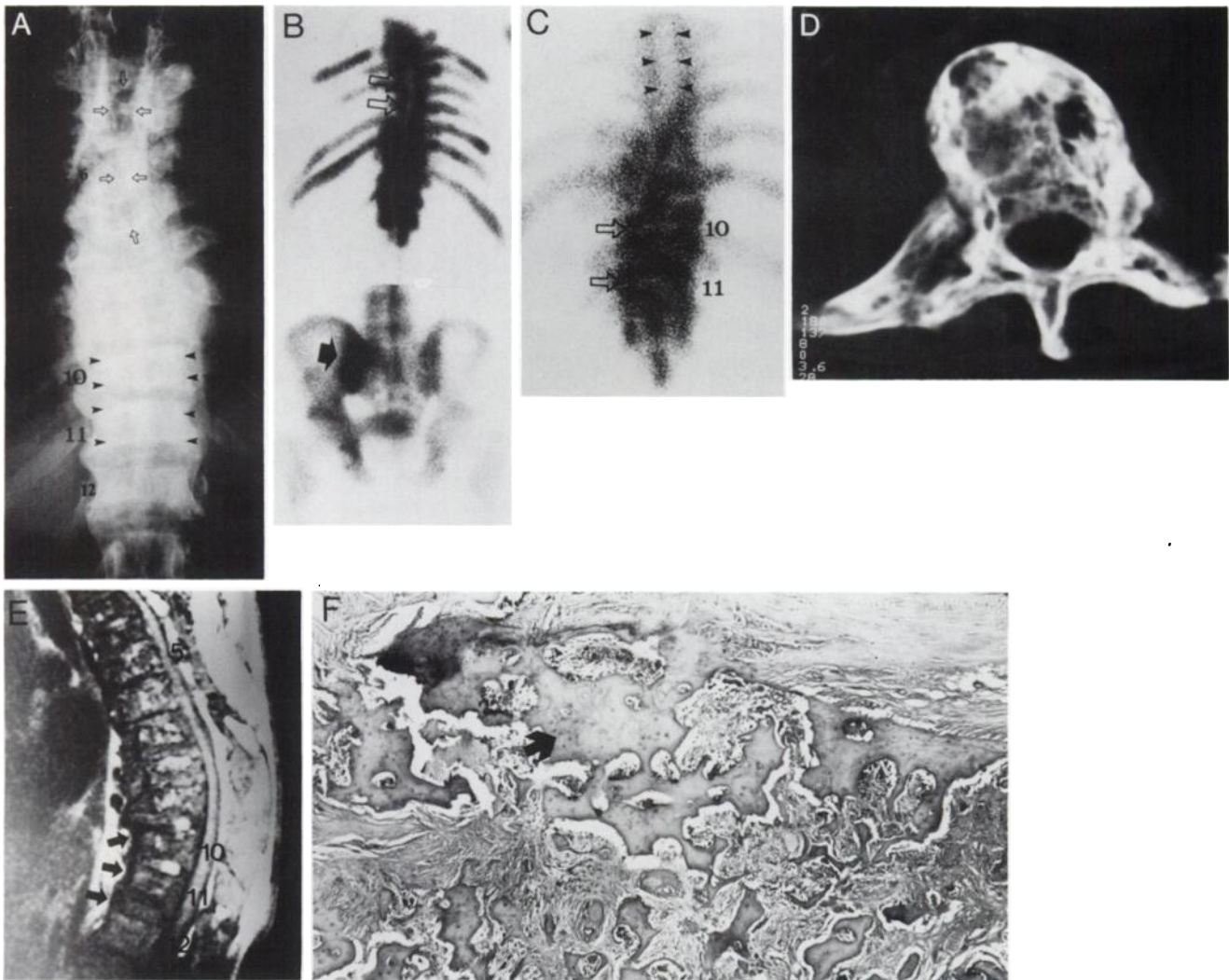


FIGURE 5. Thoracic spine in Patient 2. (A) High kV anteroposterior radiographic view reveals diffuse sclerosis in the mid- and lower thoracic spine and some of the ribs. The endplates and lateral cortices of T10 and T11 are sclerotic, producing the picture frame sign (arrowheads). T9 is compressed and a large midline surgical bone defect is seen in T4-T7. (B) Composite high-resolution posterior spot view of the spine and pelvis shows intense tracer uptake in the thoracic spine, ribs and left medial ilium (arrow). The uptake is simply homogeneous without textural details. There is a barely visible, photopenic, surgical defect (open arrows). (C) Posterior PBS portrays intense tracer uptake in T10 and T11 indicate preferential uptake in the thickened endplates and lateral cortices (open arrows). The laminectomy defect is also distinctly delineated (arrowheads) and diffuse and segmental uptake areas are clearly seen in the ribs. T9 is compressed. (D) Transaxial CT scan of T10 reveals bizarre, trabecular thickening with the most pronounced change occurring in the rim. (E) T1-weighted midsagittal MRI shows irregular, abnormal tissue depositions that have intermediate and fat signal intensities. Normal marrow signal is absent and the rims are thickened in T10-T12 (arrows). Low signal intensities in these vertebrae correspond to the radiographic picture frame sign. The compression fracture is evident in T9. (F) Low magnification photomicrograph of the cortical bone secured by excision biopsy from lower thoracic vertebra shows bone resorption, classic mosaic pattern of cement lines (arrow), haphazard new bone formation and fibrotic marrow (bottom). The periosteum is in the top (H&E; 100 \times).

scan, pinhole bone scintigraphy and radiography were performed supplementally. Pinhole bone scintigraphy visualized a large area of moderately intense tracer uptake in the medial aspect of the left iliac bone along the sacroiliac joint. It was surrounded by more intense marginal uptake, producing a rimmed appearance (Fig. 6A). Radiographs showed a comparable lytic lesion with sclerotic margin on the auricular surface (Fig. 6B). On the basis of these imaging studies, a diagnosis of Paget's disease was made. The spinal lesion was reopened for a second look. Excisional biopsies taken from the lower thoracic vertebrae showed the classic mosaic pattern of remodeling pagetic bone with brisk bone resorption and formation and replacement of cortex and marrow (Fig. 5F).

DISCUSSION

Pathologically, the pagetic bone in an active phase of the disease is characterized by brisk osteoclastic and osteoblastic activities with trabecular resorption and accretion, increased vascularity and the replacement of marrow with pagetic tissues (2,7,21). In the cranium, the diploe and tables are affected with lysis and sclerosis, especially in the frontal and occipital bones, resulting in the alterations described as osteoporosis circumscripta and the cotton wool sign. On the other hand, in the long and irregular bones,

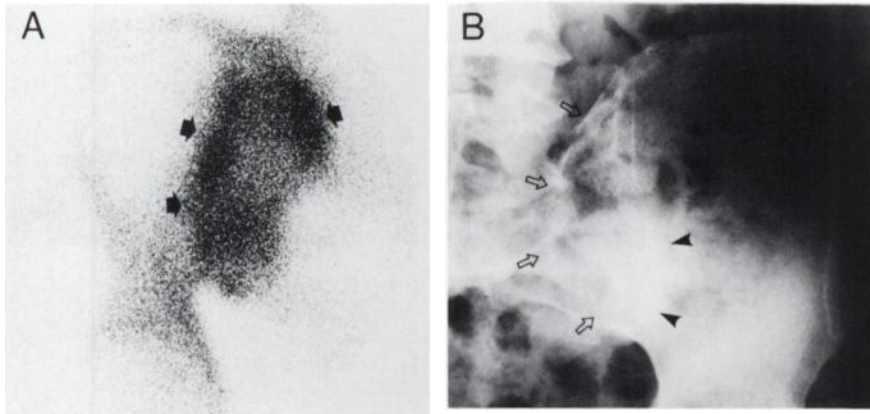


FIGURE 6. Left ilium in Patient 2. (A) Posterior pinhole bone scan portrays a large area of intense tracer uptake in the medial aspect of the ilium. The lesion is well demarcated by more intense uptake in the tuberosity (single arrow) and along the lateral border (double arrows). (B) Anteroposterior radiographic view shows a large, ill-defined area of lysis in the auricular surface. The iliac tuberosity is lytic (open arrows) and the lateral border sclerotic (arrowheads). There is close correlation between pinhole and radiographic findings.

abundant spongy bone may form at the periosteal surface, producing pumice bone in the bone peripheries (2,22). In general, the disease that typically starts from one bone end and progresses to the other more regularly involves the skull, spine, ribs, pelvis, humerus and femur.

On radiography and CT, lysis and sclerosis are, respectively, indicated by the loss of and increase in the size of trabeculae (1,23-25). The affected bones may be enlarged and the marrow space encroached. As previously mentioned, osteoporosis circumscripta and cotton-wool sign are two well-known radiographic signs of the pagetic skull, denoting exuberant lysis and new bone formation, respectively (Fig. 2B). In the long bone, lysis is often indicated by a V-shaped defect and porous sclerosis by pumice bone (Fig. 3B). When the vertebrae are affected, picture frame signs may be produced due to the thickening of the endplates and rim (Fig. 5A). MRI alterations of pagetic bone include intermediate signal intensities of pagetic tissues and irregularly interspersed high signal intensities of fat (Fig. 2C and 5E) (23,25).

Planar or spot views in Paget's disease reveal intense tracer uptake in the axial and limb bones (Figs. 1 and 5B). The extreme intensity of uptake has been pointed out, as a helpful finding (6,10), but it is not specific. By contrast, pinhole bone scintigraphy specifically portrays intense and preferential tracer accumulation in the cortex (Figs. 2A, 3A, 4A, 5C and 6A). From a diagnostic standpoint, such preferential accumulation is significant because it reflects the characteristic, pathologic features of Paget's disease. Thus, our pinhole bone scintigraphy studies showed that the tracer characteristically accumulates in the inner table and diploe of the frontoparietal bones (Fig. 2A), humeral cortex (Fig. 3A), crests, spinous tubercles, foraminal margins and sacral edges (Fig. 4A), the vertebral endplates and rims (Fig. 5C) and the auricular margins of the ilium (Fig. 6A). Interestingly, tracer uptake in the frontal bone resembled the radiographic cotton wool sign (Fig. 2A,B) and uptake in the humerus and vertebrae resembled the casket (Fig. 3A,B) and picture frame signs (Fig. 5A,C), respectively. In addition, as described by Rausch et al. (5), extremely intense marginal uptake in the skull and in the iliac

lesion seemed to reflect the advancing front of the lytic foci of Paget's disease (Figs. 2A and 6A).

CT was valuable in assessing trabecular alterations in Paget's disease (Fig. 5D) (24,25) and MRI uniquely showed the changes in signal intensities due to pagetic tissues and fat deposition (Figs. 2C and 5E) (24,26). A comparison of the radiographic and pinhole bone scintigraphic findings of the pagetic skull in Patient 1 showed good correlation between the cotton wool sign and localized, intense tracer uptake (Fig. 2A,B). In turn, these findings correlated well with those of MRI (Fig. 2C). Similar results were obtained from a cross-correlation study of pinhole bone scintigraphy, radiography, CT and MRI of the pagetic vertebrae in Patient 2 (Fig. 5A,C,D,E). The excisional biopsies from the vertebral cortex confirmed typical pagetic bone changes in the subperiosteal layer (Fig. 5F).

In conclusion, preferential tracer uptake in the cortex and rim of bone lesions denotes brisk bone formation and lysis that characterize Paget's disease.

ACKNOWLEDGMENTS

The authors thank Mr. Hyung Koo Cho, Mr. Sang Mok Lee and Mr. Byung Hak Kim for technical assistance, and Ms. Hee Sup Choi for secretarial assistance. This work was supported in part by the Clinical Research Fund of Catholic University Medical College and Center, Seoul, Korea.

REFERENCES

1. Resnick D, Niwayama G. Paget's disease. In: Resnick D, Niwayama G, eds. *Diagnosis of bone and joint disorders*, 2nd Ed. Philadelphia: WB Saunders; 1988:2127-2179.
2. Revel PA. Paget's disease of bone. In: *Pathology of bone*. Berlin: Springer-Verlag; 1986:147-167.
3. Wellman NH, Schaurwecker D, Robb JA, et al. Skeletal scintimaging and radiography in the diagnosis and management of Paget's disease. *Clin Orthop* 1977;127:55-62.
4. Miller SW, Castronova, Jr FP, Pendergrass HP, Potsaid MS. Technetium-99m labeled diphosphonate bone scanning in Paget's disease. *AJR* 1974;121:177-183.
5. Lentle BC, Russell AS, Heslip PG, Percy JS. The scintigraphic findings in Paget's disease of bone. *Clin Radiol* 1976;27:129-135.
6. Rausch JM, Resnick D, Goergen TG, Taylor A. Bone scanning in osteolytic Paget's disease: case report. *J Nucl Med* 1977;18:699-701.
7. Frame B, Marel GM. Paget disease: a review of current knowledge. *Radiology* 1981;141:21-24.

8. Waxman AD, Ducker S, McKee D, Siemsen JK, Singer FR. Evaluation of ^{99m}Tc diphosphonate kinetics and bone scans in patient with Paget's disease before and after calcitonin treatment. *Radiology* 1977;125:761-764.
9. Vellenga CJLR, Pauwels EKJ, Bijvoet OLM, Frijlink WB. Scintigraphic aspects of the recurrence of treated Paget's disease of bone. *J Nucl Med* 1981;22:510-517.
10. Serafini AN. Paget's disease of the bone. *Semin Nucl Med* 1976;6:47-58.
11. Burgener FA, Kormano M. Osteosclerosis. In: *Differential diagnosis in conventional radiology*. Stuttgart: Thieme; 1991:13-31.
12. Bahk YW. The usefulness of pinhole scintigraphy in bone and joint diseases. *Jpn J Nucl Med* 1982;19:1307.
13. Bahk YW. Usefulness of pinhole collimator scintigraphy in the study of bone and joint diseases. In: Britton KE, ed. *Proceedings of Nuclear Medicine Congress: Europe*. London: European Society of Nuclear Medicine; 1985:262.
14. Bahk YW, Kim OH, Chung SK. Pinhole collimator scintigraphy in differential diagnosis of metastasis, fracture and infections of the spine. *J Nucl Med* 1987;28:447-451.
15. Bahk YW. Pinhole scintigraphic and radiographic imaging of inflammatory bone and joint diseases. In: Masjhur JS, ed. *Precongress teaching course*. Fifth Asia and Oceania Congress of Nuclear Medicine. Jakarta-Bali: Asia and Oceania Society of Nuclear Medicine and Biology; 1992:19-35.
16. Bahk YW, Chung SK, Kim SH. Pinhole scintigraphic manifestations of sternocostoclavicular hyperostosis. *Korean J Nucl Med* 1992;26:155-159.
17. Kim JY, Chung SK, Park YH, Kim SH, Bahk YW. Pinhole bone scintigraphic appearances of osteoid osteoma. *Korean J Nucl Med* 1992;26:160-163.
18. Kim SH, Chung SK, Bahk YW. Pinhole scintigraphic demonstration of septation in metastatic thyroid carcinoma in bone. *Korean J Nucl Med* 1993;27:305-308.
19. Bahk YW, Park YH, Chung SK, Kim SH, Shinn KS. Pinhole scintigraphic sign of chondromalacia patellae in aged subjects: a prospective assessment with differential diagnosis. *J Nucl Med* 1994;35:855-862.
20. Yang WJ, Bahk YW, Chung SK, Choi KH, Jo KH, Jee MK. Pinhole scintigraphic manifestations of Tietze's disease. *Eur J Nucl Med* 1994; 21:947-952.
21. Bahk YW. *Combined scintigraphic and radiographic diagnosis of bone and joint diseases*. Heidelberg: Springer-Verlag; 1994.
22. Jaffe H. *Metabolic, degenerative, and inflammatory disease of bones and joints*. Philadelphia: Lea & Febiger; 1972:240-271.
23. Edeiken J, Dalinka M, Karasick D. *Edeiken's Roentgen diagnosis of diseases of bone*, 4th Ed. Baltimore: Williams and Wilkins; 1990:1231-1259.
24. Roberts MC, Kressel HY, Fallon MD, Zlatkin MB, Dalinka MK. Paget disease: MR imaging findings. *Radiology* 1989;173:341-345.
25. Zlatkin MB, Lander PH, Hadjipavlou AG, Levine JS. Paget disease of the spine: CT with clinical correlation. *Radiology* 1986;160:155-159.
26. Firooznia HF. Paget's disease. In: Firooznia HF, Golimbu C, Rafii M, Rauschnig W, Weinreb J, eds. *MRI and CT of the musculoskeletal system*. St. Louis: Mosby-Year Book; 1992:176-181.